

Minerva Access is the Institutional Repository of The University of Melbourne

Author/s:

Jörg, M;Agostino, M;Yuriev, E;Mak, FS;Miller, ND;White, JM;Scammells, PJ;Capuano, B

Title:

Synthesis, molecular structure, NMR spectroscopic and computational analysis of a selective adenosine A2A antagonist, ZM 241385

Date:

2013-08-01

Citation:

Jörg, M., Agostino, M., Yuriev, E., Mak, F. S., Miller, N. D., White, J. M., Scammells, P. J. & Capuano, B. (2013). Synthesis, molecular structure, NMR spectroscopic and computational analysis of a selective adenosine A2A antagonist, ZM 241385. *Structural Chemistry*, 24 (4), pp.1241-1251. <https://doi.org/10.1007/s11224-012-0151-7>.

Persistent Link:

<https://hdl.handle.net/11343/282665>

Draft submission for review to **SPRINGER PUBLISHING****Synthesis, molecular structure, NMR spectroscopic and computational analysis of a selective adenosine A_{2A} antagonist, ZM 241385****Manuela Jörg · Mark Agostino · Elizabeth Yuriev · Frankie S. Mak · Neil D. Miller · Jonathan M. White · Peter J. Scammells · Ben Capuano**Manuela Jörg · Mark Agostino · Elizabeth Yuriev · Peter J. Scammells · Ben Capuano
(corresponding author)Medicinal Chemistry, Monash Institute of Pharmaceutical Sciences, 381 Royal Parade, Parkville,
VIC 3052, AustraliaE-mail: ben.capuano@monash.edu

Frankie S. Mak · Neil D. Miller

GlaxoSmithKline, GSK R&D China, Singapore Research Centre, 11 Biopolis Way, Helios Bldg
#03-01/02, Singapore 138667

Jonathan M. White

Bio21 Molecular Science & Biotechnology Institute, 30 Flemington Road, The University of
Melbourne, Parkville, VIC 3010, Australia

Mark Agostino

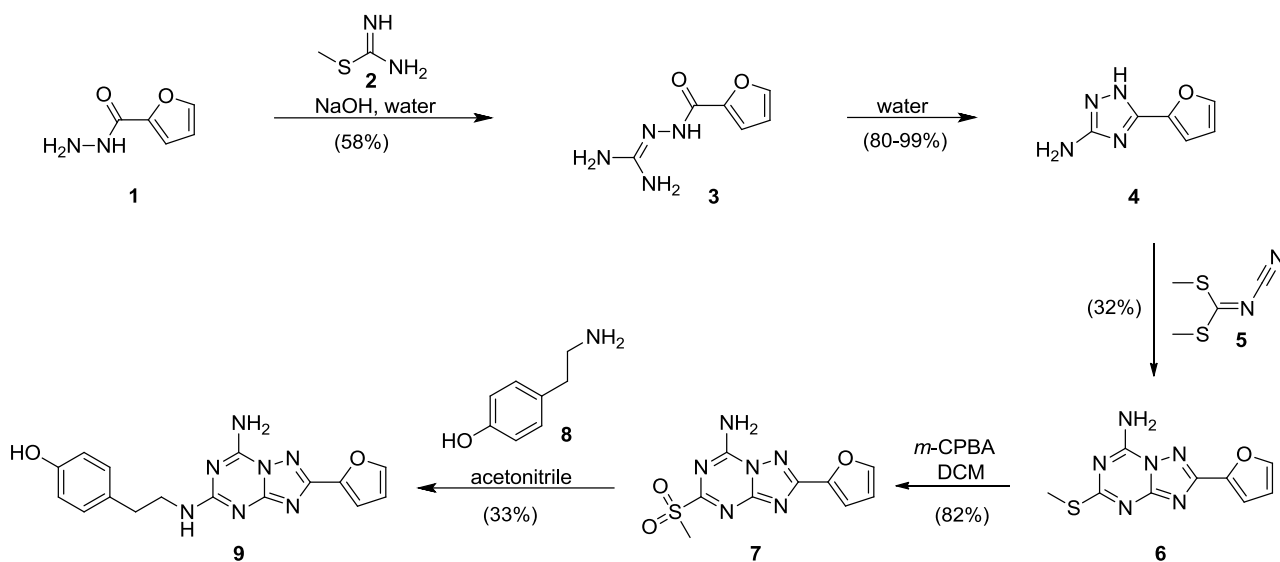
Western Australian Biomedical Research Institute, Curtin Health Innovation Research Institute,
School of Biomedical Sciences, Curtin University, GPO Box U1987, Perth WA 6845, Australia**Keywords** ZM 241385 · A_{2A} antagonist · synthesis · spectroscopic analysis · crystal structure**Abstract** Herein we describe the synthesis of the adenosine A_{2A} antagonist ZM 241385 (**9**) starting from commercially available 2-furanhydrazide (**1**) and including a comprehensive structural characterization of all the intermediates and the final product. In addition, extensive NMR analysis, including temperature and concentration-dependent experiments, are reported as well as the first single crystal structure of the compound ZM 241385 (**9**) as the trihydrate. Furthermore, an extensive structural comparison of the single crystal structure with the published protein bound x-ray structure is reported.

37 Introduction

38 The recent interest in the adenosine A_{2A} receptor as a therapeutic target has significantly increased
39 following studies that revealed that co-administration of an A_{2A} antagonist with a D₂ agonist
40 showed promising clinical efficacy in the treatment of dyskinesias associated with Parkinson's
41 disease therapy[1-3]. ZM 241385 (**9**) is a potent and selective adenosine A_{2A} antagonist [4] and the
42 first ligand for which x-ray structures in complex with the adenosine A_{2A} receptor have been solved
43 [5,6]. The molecule exhibits a distinctive 2-(furan-2-yl)-[1,2,4]triazolo[1,5-*a*][1,3,5]triazin-7-amine
44 scaffold and has been extensively used as a lead compound for various structure-activity
45 relationship studies [2,7,8]. Nevertheless, limited experimental data and no comprehensive
46 structural characterization (including x-ray crystal structure) or analysis of the NMR spectral
47 characteristics has been published to date. Furthermore, the comparison of the two published
48 protein bound x-ray structures showed some interesting differences which will be discussed later.

50 Synthesis

51 ZM 241385 (**9**) was synthesised according to the pathway illustrated in Scheme 1. The original
52 patent synthesis of ZM 241385 [4] commenced with the precursor compounds aminoguanidine
53 nitrate and 2-furonitrile. Our modified synthesis, although comparable with literature, commenced
54 with commercially available 2-furanhydrazide (**1**) and incorporates relatively inexpensive reagents.



56
57 **Scheme 1** Chemical synthesis of ZM 241385 (**9**).

58
59 A mixture of furan-2-carbohydrazide (**1**), *S*-methylisothiourrea (**2**) and sodium hydroxide in water
60 was stirred at room temperature for 14 hours and following work-up gave the
61 furanoylhydrazinecarboximidamide intermediate **3** in a moderate yield of 58%. The yield obtained

62 was consistent with that observed in the literature (52% yield) [9]. The following step was
63 accomplished by employing one of two methods published by Dolzhenko *et al.* [10], depending on
64 reaction scale. On a scale up to 1 g, intermediate **3** was suspended in water and the reaction was
65 performed in the microwave at 140 °C for 1 h before the solvent was removed under vacuum. The
66 yield for this method was virtually quantitative (99%). On a larger scale, the reaction of the aqueous
67 suspension was performed using conventional heating at 100 °C for 29 h. The reaction volume was
68 reduced and the precipitate filtered. Yields up to 80% were achieved via the second method. 5-
69 (Furan-2-yl)-1*H*-1,2,4-triazol-3-amine (**4**) was reacted with *N*-cyanodithioiminocarbonate (**5**) to
70 afford **6** in 32% yield after column chromatography [4,11]. The sulfide intermediate **6** was
71 subsequently oxidized with *m*-chloroperoxybenzoic acid at room temperature to afford the sulfone **7**
72 in excellent yield (82%) [11,4]. Nucleophilic displacement of the methylsulfonyl group with
73 tyramine (**8**) [4] furnished the target triazolotriazine (**9**, ZM 241385) in a 33% yield with purity
74 greater than 97% as determined by analytical HPLC.

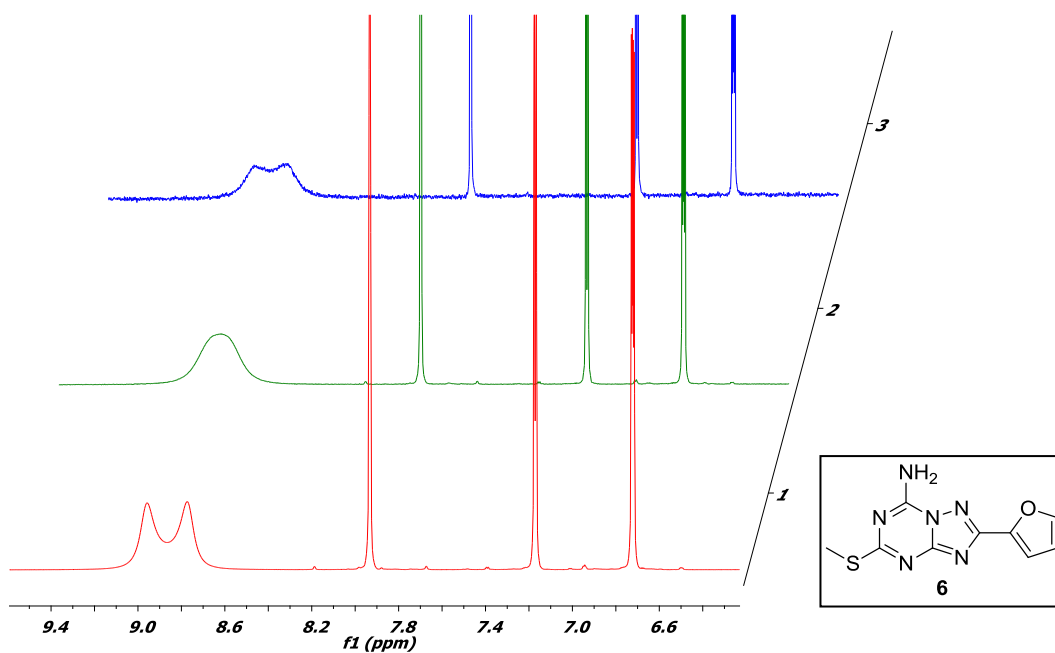
75

76 NMR Analysis

77 Intermediates **6** and **7** as well as the final compound ZM 241385 (**9**) showed very interesting and
78 somewhat unexpected features in their respective NMR spectra. In this section, a number of NMR
79 experiments are presented and the respective findings and interpretations are summarized and
80 evaluated. Initially, we expected a broad singlet for the hydrogens of the NH₂ group for compounds
81 **6** and **7** in the ¹H-NMR, however, two broad singlets in a 1:1 ratio were actually observed (Fig. 1
82 and 2). Caulkett *et al.* [11] observed the same phenomenon and demonstrated that the splitting was
83 temperature-dependent; at 373 K the doublet coalesced to one singlet. In the case of compound **6**,
84 we performed dilution experiments that showed the signal shape of the primary amine to be
85 dependent on the concentration of the sample. Fig. 1 shows two broad singlets (8.7-9.2 ppm) with a
86 sample concentration of 7 mg/mL, one broad singlet at 1 mg/mL and again two broad singlets at
87 0.1 mg/mL. Dilution experiments (Fig. 2) were also performed with molecule **7**, but the signals
88 never coalesced. Interestingly, when the compound [1,2,4]triazolo[1,5-*a*][1,3,5]triazin-7-amine (**10**)
89 (Fig. 3) was analysed under the same conditions, it did not exhibit any doubling up of the amino
90 signal at any concentration.

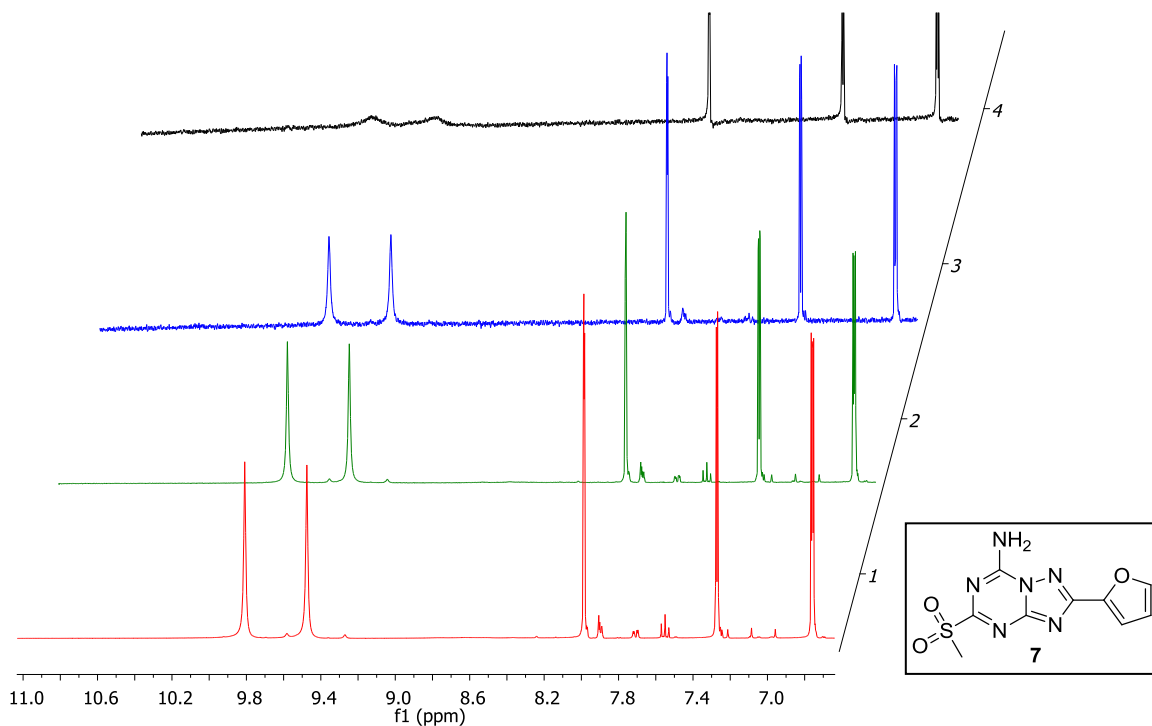
91

92



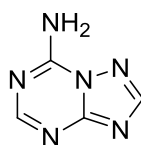
93
94
95
96
97
98

Fig. 1 Section of the ^1H NMR spectrum of compound **6** which shows the NH_2 signals and the three furyl protons at a sample concentration of 7 mg/mL (red, spectrum 1), 1 mg/mL (green, spectrum 2) and 0.1 mg/mL (blue, spectrum 3).



99
100
101
102
103

Fig. 2 Section of the ^1H NMR spectrum of compound **7** which shows the NH_2 signals and the three furyl protons at a sample concentration of 7 mg/mL (red, spectrum 1), 1 mg/mL (green, spectrum 2), 0.1 mg/mL (blue, spectrum 3) and 0.01 mg/mL (black, spectrum 4).



10

Fig. 3 Chemical structure of [1,2,4]triazolo[1,5-*a*][1,3,5]triazin-7-amine (**10**).

The NMR spectra of ZM 241385 (**9**) not only exhibited splitting of the proton signals in the ^1H NMR spectrum, but also splitting of the carbon signals in the ^{13}C NMR spectrum. The NH_2 and NH groups of ZM 241385 (**9**) in the ^1H NMR spectrum in d_6 -DMSO each displayed two signals in a ratio of 1:6 and 1:2, respectively. Fig. 4 shows that the amino signals coalesced at 353 K into one broad singlet and one broad triplet for the NH_2 and NH groups, respectively. The splitting patterns of the CH_2 signals of the tyramine moiety in the proton spectrum also exhibit greater resolution at 353 K compared to 298 K.

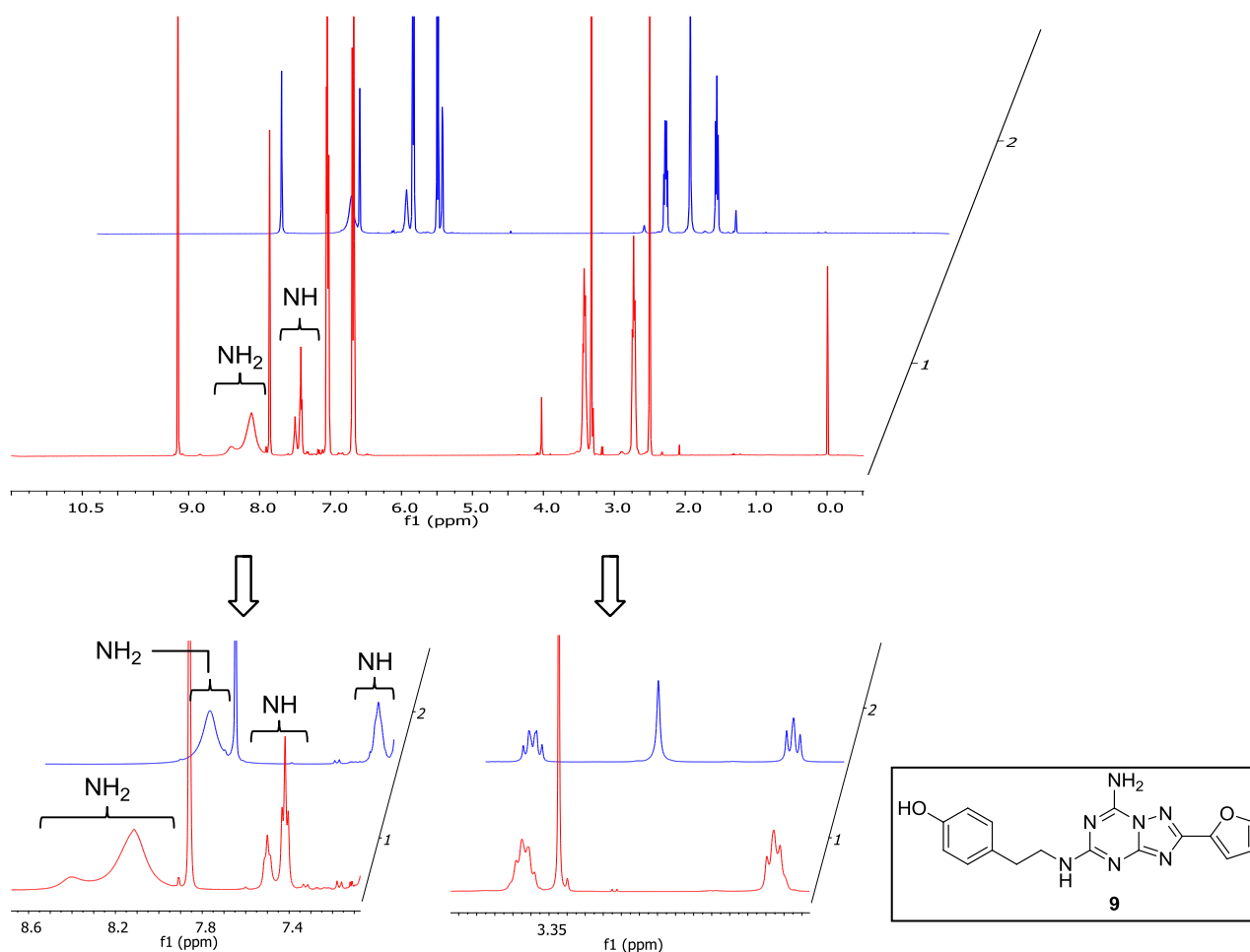
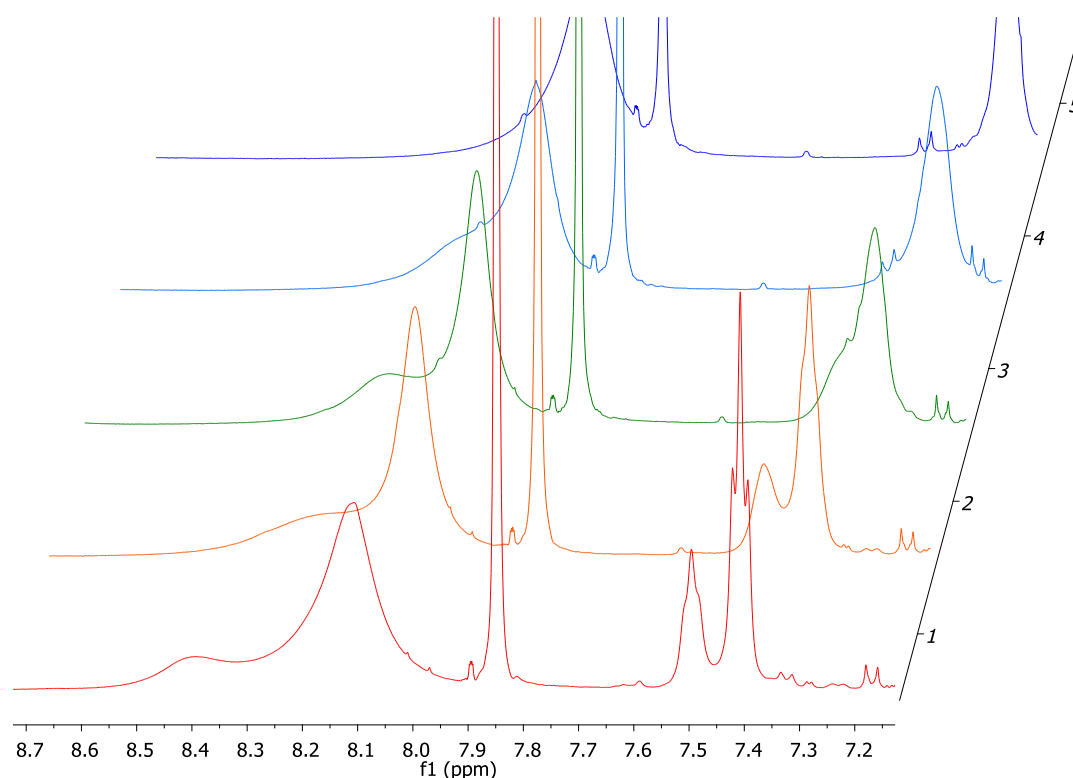


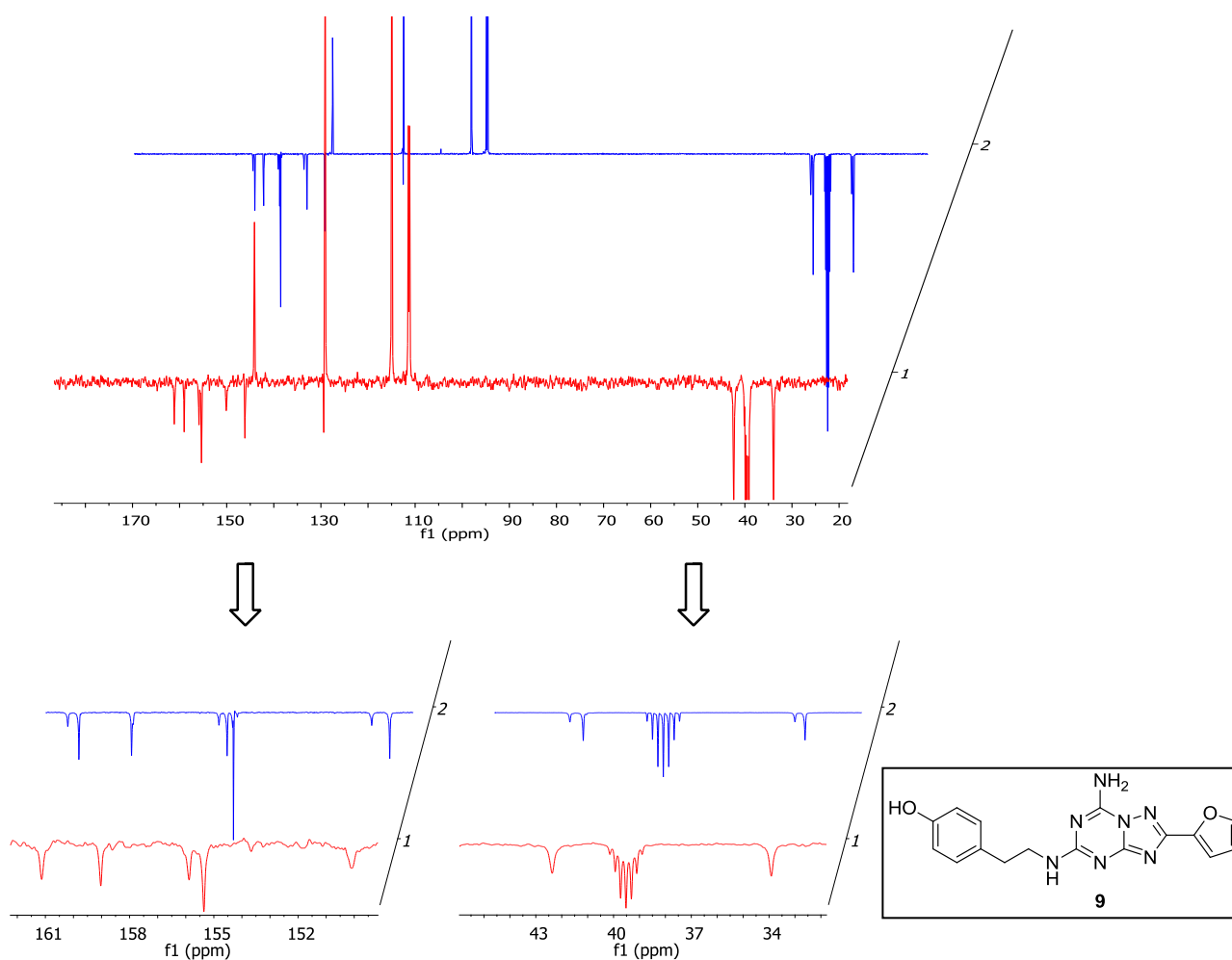
Fig. 4 ^1H NMR spectrum of ZM 241385 (**9**) at 298 K (red, spectrum 1) and 353 K (blue, spectrum 2) (upper). The lower left spectrum shows a zoomed section of the amino protons, that each show two signals at 298 K and one signal at 353 K. The lower right spectrum shows the CH_2 signals of the tyramine moiety at 298 K and 353 K.

120 Figure 5 shows the amino group resonances in the ^1H NMR spectra at different temperatures. A
121 closer look revealed that the ratio of the two signals did not change but rather the two signals moved
122 closer together until they finally coalesced. At 303 K (red spectrum), the two signals are clearly
123 observed for each of the two amino groups (NH_2 and NH). By heating the sample in 10 K
124 increments, the signals slowly moved closer together until they completely coalesced at 343 K.
125
126



127
128 **Fig. 5** ^1H NMR section of ZM 241385 (**9**) showing the amino protons at different temperatures (red = 303 K, spectrum
129 1; orange = 313 K, spectrum 2; green = 323 K, spectrum 3; light blue = 333 K, spectrum 4; dark blue = 343 K, spectrum
130 5). At 7.85 ppm is a singlet from an aromatic proton.

131
132 Unlike compounds **6** and **7**, for which no spectral anomalies were observed in their respective
133 ^{13}C NMR spectra, the title compound ZM 241385 (**9**) showed doubling up of most carbon signals.
134 This effect was observed in both d_4 -methanol and in d_6 -DMSO. The doubled-up carbon signals also
135 exhibited a temperature-dependence whereby they coalesced at 353 K (Fig. 6, blue spectrum).
136



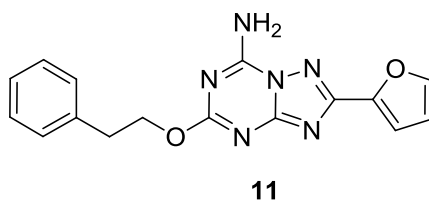
137

138 **Fig. 6** ^{13}C NMR spectra of ZM 241385 (**9**) at 298 K (blue, spectrum 1) and 353 K (red, spectrum 2) (upper). The lower
 139 left spectrum shows a zoomed section of some of the quaternary carbons at 298 K and 353 K. The lower right spectrum
 140 shows the CH_2 signals of the tyramine moiety that each show two signals at 298 K and a single resonance at 353 K.

141

142 Interestingly, the 2-(furan-2-yl)-5-phenethoxy-[1,2,4]triazolo[1,5-*a*][1,3,5]triazin-7-amine (**11**),
 143 which contains a phenethoxy moiety instead of the tyramine moiety, also exhibited doubling up of
 144 the amino group signal at position 7 in a 1:1 ratio, however, no anomalies were observed in the ^{13}C -
 145 NMR spectrum.

146



147

148 **Fig. 7** Structure of 2-(furan-2-yl)-5-phenethoxy-[1,2,4]triazolo[1,5-*a*][1,3,5]triazin-7-amine (**11**).

149

150 The splitting of the amino signal was not observed for compound **10**, therefore intramolecular
 151 interactions such as hydrogen bonding are unlikely to explain this phenomenon for intermediates **6**

152 and **7**. Tautomerism was excluded due to the observations that (i) no additional carbon signals were
153 observed, (ii) no additional cross peaks were present in the ^{15}N - ^{13}C HQMC and (iii) that it would be
154 very unlikely to observe an exact 1:1 ratio of the amino signals for both compounds **6** and **7**. The
155 fact that the signals in molecules **6** and **7** appear in exactly a 1:1 ratio, in addition to the observed
156 temperature and concentration dependency, indicates that intermolecular interactions, such as
157 dimer formation, are likely to be responsible for the observed doubling up of the amino group
158 resonances.

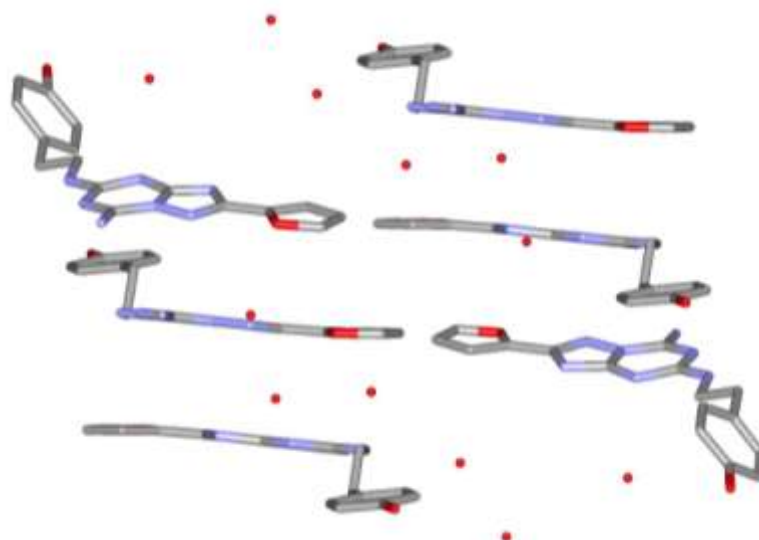
159 In the case of the literature compound ZM 241385 (**9**), the spectral phenomena are more complex
160 and we propose that this is due to the two effects occurring simultaneously, namely intermolecular
161 interactions, such as dimer formation in conjunction with hindered rotation at the secondary amino
162 group of the tyramine moiety. A comparison between molecules **9** and **11**, shows that removing the
163 secondary amine on the ligand in position 2 affects the ratio of the signals but not the doubling up
164 effect. This indicates that intermolecular interactions still occur but the second underlining effect
165 has been eliminated. Some publications have examined similar effects caused either by nitrogen
166 inversion or hindered rotation [12-14]. In the case of ZM 241385 (**9**), nitrogen inversion seems to be
167 very unlikely due to the fact that the x-ray crystal structure of the molecule exhibits primarily sp^2
168 character for the amino group of the tyramine moiety (*vide infra*).

169

170 **X-ray structure of ZM 241385**

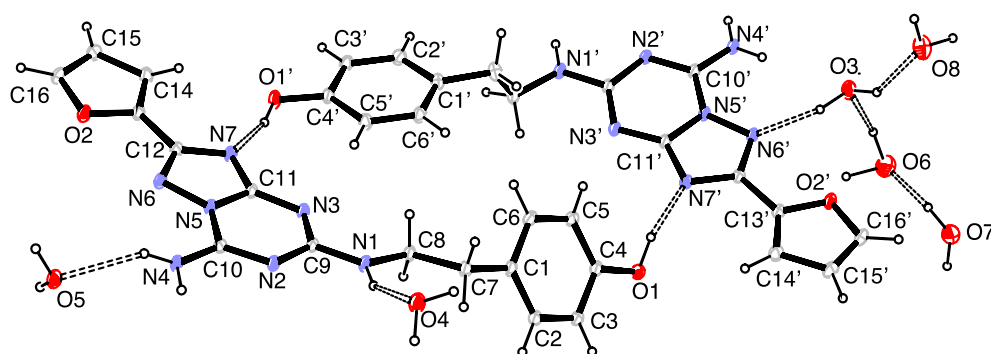
171 Crystals of the title compound **9** were grown by using a two layer system of methanol and
172 petroleum spirit. The crystals were used to generate an x-ray structure for ZM 241385 (**9**) which not
173 only proved that the correct molecule was synthesized but also gave interesting insight into the
174 crystal packing. Compound **9** crystallizes with two independent molecules, and six water molecules
175 in the asymmetric unit as displayed in Fig. 8. The two molecules form a head-to-tail arrangement
176 stabilized by hydrogen bonds (Fig. 9) between the hydroxyl groups (O1-H and O1'-H) on each
177 molecule and the triazine nitrogens (N6' and N6) (see Table 1 for a complete list of hydrogen bond
178 contacts in the crystal). The six water molecules form a cluster that helps to further stabilize the π -
179 stacked layers of the ligand (Fig. 8 and 10).

180



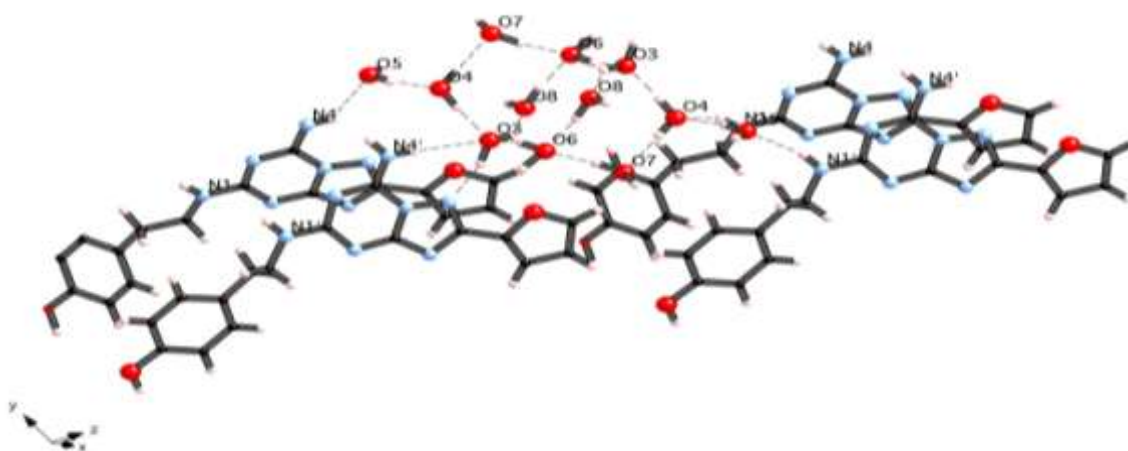
181
182
183
184

Fig. 8 Crystal packing of six ZM 241385 (**9**) molecules including water molecules (red dots).



185
186
187
188
189
190

Fig. 9 Thermal ellipsoid plot for compound **9**. Ellipsoids are at the 20% probability level.



191
192
193
194

Fig. 10 Partial packing diagram of compound **9**, showing the cluster of water molecules which helps to stabilize the crystal by forming hydrogen bond between layers of the ligand.

Table 1 Hydrogen bonds for two molecules of ZM 241385 (**9**) [\AA and $^\circ$].

D-H...A	d(D-H)	d(H...A)	d(D...A)	$\angle(\text{DHA})$
N(4)-H(4A)...O(5)	0.82(3)	2.19(3)	2.851(3)	137(2)
O(1')-H(1'B)...N(7)	0.90(4)	1.81(4)	2.689(2)	165(3)
O(1)-H(1B)...N(7')	0.96(4)	1.75(4)	2.697(2)	168(3)
N(4')-H(4'A)...O(3)	0.82(3)	2.49(3)	3.307(3)	175(2)
N(1)-H(1A)...O(4)	0.89(3)	2.21(3)	3.026(3)	153(3)
O(3)-H(3A)...N(6')	1.00(4)	1.87(4)	2.826(3)	160(3)
O(7)-H(7D)...O(6)	1.094(17)	1.831(19)	2.922(4)	175(5)
N(4)-H(4B)...N(2')#1	0.82(3)	2.13(3)	2.942(3)	172(3)
N(1')-H(1'A)...O(5)#2	0.87(3)	2.09(3)	2.927(2)	163(2)
N(4')-H(4'B)...N(2)#2	0.87(3)	2.20(3)	3.048(3)	163(2)
O(5)-H(5A)...O(1')#3	0.77(3)	2.04(3)	2.808(3)	175(3)
O(4)-H(4D)...O(3)#1	0.93(4)	1.86(4)	2.776(3)	168(3)
O(4)-H(4C)...O(7)#4	0.88(4)	1.95(4)	2.807(3)	163(3)
O(8)-H(8D)...O(6)#5	1.02(4)	1.82(4)	2.832(4)	173(5)
O(8)-H(8C)...N(3)#6	1.02(4)	2.17(5)	3.158(3)	162(6)

Symmetry transformations used to generate equivalent atoms:

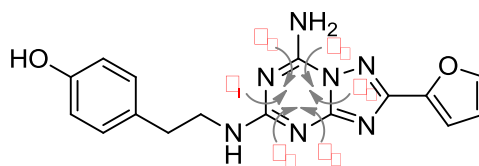
#1 $x, y+1, z+1$ #2 $x, y-1, z-1$ #3 $-x+3, -y+2, -z+3$

#4 $-x+1, -y+1, -z+1$ #5 $-x+1, -y, -z$ #6 $x-1, y-1, z-1$

The crystal structure of ZM 241385 (**9**) revealed slight puckering of the triazine portion of the heterocycle (Table 2). Ideally, the torsions within the triazine should all be 0° , reflecting the aromaticity of the structure. However, one of the crystallographically determined structures revealed differences of up to 5° from the ideal predicted geometry.

226
227

Table 2 Comparison of torsion angles within the triazine portion of the ZM 241385 heterocycle.



228

Source	Φ_1	Φ_2	Φ_3	Φ_4	Φ_5	Φ_6
PDB 3EML	1.2°	-0.8°	0.3°	0.0°	0.3°	-0.9°
PDB 3PWH	-0.1°	-0.1°	0.1°	-0.1°	0.1°	-0.1°
ZM241385 structure 1	-0.7°	6.0°	-5.2°	-1.4°	6.4°	-5.6°
ZM241385 structure 2	1.8°	-1.3°	0.4°	0.3°	0.1°	-1.2°

229

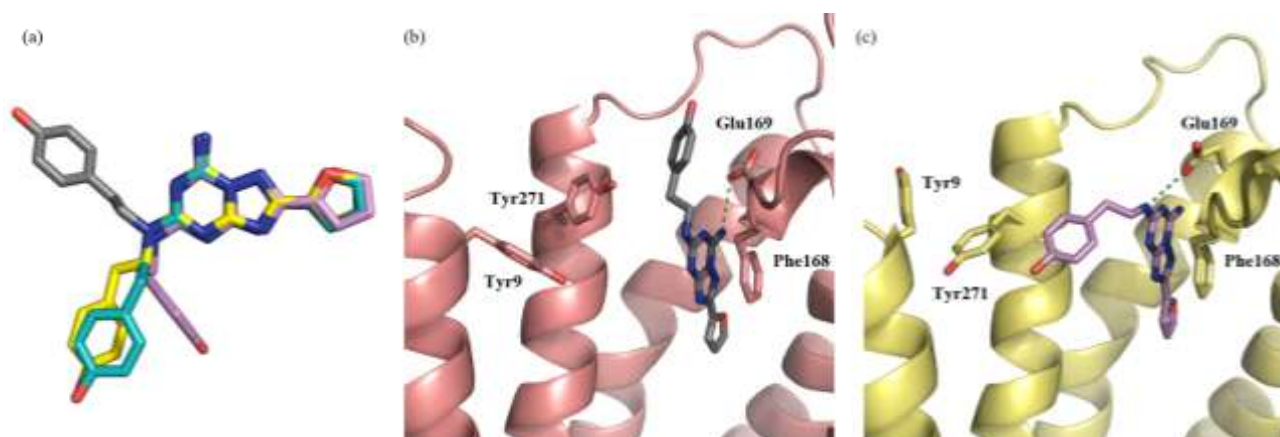
230

231 Comparison of ZM 241385 crystal structures

232 The science of producing x-ray structures of receptors in complex with specific ligands has
233 significantly improved the understanding of structure-function relationships and progressed
234 structure-based drug design to a new dimension. Nevertheless, obtaining ligand bound x-ray
235 structures in complex to G protein-coupled receptors, including the adenosine A_{2A} receptor, is still a
236 challenging task due to problems such as low thermostability and low receptor expression
237 levels [15]. In 2008, Jaakola *et al.* published the first x-ray (PDB 3EML) of the A_{2A} receptor in
238 complex with the A_{2A} antagonist ZM 241385 (**9**) which revealed a unique ligand binding pocket [5]
239 (Fig. 11b). This x-ray structure was generated using a T4 lysozyme (T4L) fusion strategy. More
240 recently Dore *et al.* published a second receptor bound x-ray (PDB 3PWH) structure of ZM 241385
241 (**9**) by using a thermostabilized adenosine A_{2A} receptor [6] (Fig. 11c). The two x-ray structures
242 show subtle differences in their respective ligand interactions with the receptor, namely i) the ligand
243 is placed slightly deeper into the binding site in 3EML compared to 3PWH, and ii) the
244 conformation of tyrosine residues (Tyr9 and Tyr271 in the PDB sequences) near the phenol moiety
245 of ZM 241385 (**9**) changes dramatically between the two structures (Fig. 11b and 11c).
246 Consequently, the adenosine receptor has space to accommodate the inherent flexibility of the
247 tyramine moiety.

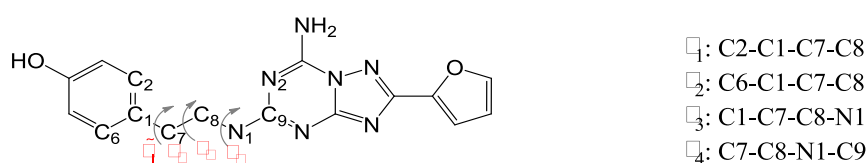
248 Herein we extensively compare the ZM 241385 (**9**) coordinates obtained from the two available
249 crystal structures of the ligand in complex with the adenosine A_{2A} receptor [5,6] with that of the
250 unbound crystal structure of ZM 241385 (**9**), presented here (two molecules per unit cell).

251



252
 253 **Fig. 11** (a) Overlay of four ZM 241385 structures. Yellow carbons – ZM 241385 structure 1; teal carbons – ZM 241385
 254 structure 2; grey carbons – ZM 241385 in complex with A_{2A} receptor (PDB 3EML); violet carbons – ZM 241385 in
 255 complex with A_{2A} receptor (PDB 3PWH). (b) ZM 241385 (violet) in complex with A_{2A} receptor/lysozyme fusion
 256 (yellow) (PDB 3EML). (c) ZM 241385 (grey) in complex with thermostabilized A_{2A} receptor (pink) (PDB 3PWH).
 257 Transmembrane helices 2 and 3 removed from figures of complex structures for clarity. Blue and red colors represent
 258 oxygen and nitrogen atoms, respectively.
 259

260 **Table 3** Comparison of torsion angles for the tyramine portion of ZM 241385 (**9**).



Source	τ_1/τ_2	τ_3	τ_4
PDB 3EML	-43.2° / 135.7°	-176.1°	91.6°
PDB 3PWH	-165.7° / 14.0°	140.4°	107.8°
ZM 241385 structure 1	-70.3° / 110.7°	-171.1°	-167.9°
ZM 241385 structure 2	-68.8° / 112.7°	159.3°	89.5°

262
 263 The overlay of the four ZM 241385 (**9**) structures revealed that the tyramine portion of the ligand
 264 can adopt different conformations depending on the structural context (Fig. 11a, Table 3). Most
 265 interestingly, the adenosine A_{2A} receptor appears to be able to recognize two strikingly different
 266 conformations of this portion of the tyramine moiety; this was previously noted by Doré et al [6].
 267 The two structures from the unbound crystal structure of ZM 241385 (**9**) adopted slightly different
 268 conformations of the tyramine portion of the ligand, which resided in between the two extremes of
 269 the structures obtained by Doré et al. and Jaakola et al [16]. As shown in Fig. 11b and 11c, the
 270 conformation of Glu169 also changes between the two crystal structures, resulting in hydrogen

271 bonds in different locations of ZM 241385. Phe168 engages in π -stacking with the purine-like
272 heterocycle in both cases.

273

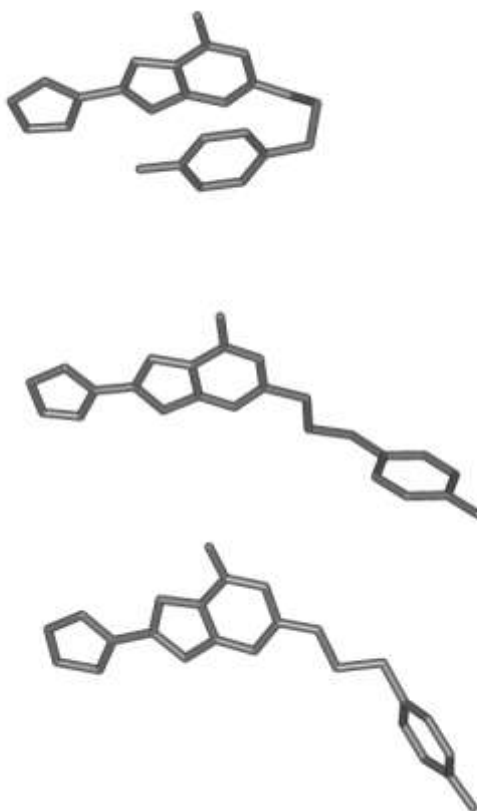
274 **Vacuum and explicit aqueous solution conformational searches**

275 Variations in the conformations of the bound ZM 241385 (**9**) and their comparison to the
276 conformations of the unbound compound point to its extensive flexibility. In order to further
277 address this issue we have extended the structural analysis of ZM 241385 (**9**) and carried out
278 conformational searches for this compound *in vacuo* and in explicit aqueous solution.

279 Compound ZM 241385 (**9**) contains a flexible linker, connecting two rigid moieties; a substituted
280 benzene ring and a heterocyclic triazolotriazine ring system. The furan and triazolotriazine rings,
281 the linker itself, as well as the hydroxyl substituent on the aromatic ring make this molecule fairly
282 hydrophilic. Thus due to these properties and to the flexibility of the linker, the two ring systems
283 have the ability to interact via intramolecular van der Waals (vdW) and hydrogen bonding
284 interactions, thus potentiating a range of accessible conformations, depending on the environment
285 (Fig. 12).

286 The lowest energy structure obtained from the conformational search of ZM 241385 (**9**) *in vacuo*
287 featured the phenol portion of the ligand stacking with the heterocycle (Fig. 12 [top]). In solution,
288 two main forces determine the preferred conformation. On one hand, intramolecular vdW and
289 hydrogen bonding interactions favour formation of folded conformations, so as to minimize contact
290 with water for the hydrophobic parts of the molecule (e.g., aromatic ring). On the other hand, the
291 polarizable groups (e.g., hydroxyl) ‘push’ the molecule into bulk solvent, thus aiding the extended
292 form of the compound. While both conformations have been observed in the conformational search
293 carried out in an explicit aqueous environment, the lowest energy conformation was found in the
294 extended state (Fig. 12 [middle]). This conformation is very similar to that in the solid state, except
295 for the torsion angles in the highly flexible linker. The extended conformation of the solid state
296 (Fig. 12 [bottom]) is likely to be a result of the intermolecular interactions in the crystal lattice
297 (discussed above). We have previously observed similar environment-dependent conformational
298 behavior for other molecules containing rigid hydrophobic elements decorated with polarizable
299 groups, and connected by flexible linkers [20-22].

300



302

303 **Fig. 12** Conformations of ZM 241385 in different environments. (Top) vacuum (modelled); (Middle) explicit aqueous
304 solution (modelled); (Bottom) solid state (experimental).

305

306 **Conclusion**

307 ZM 241385 (**9**) has been successfully synthesized in an overall yield of 5%. A complete
308 characterization of ZM 241385 (**9**) and its intermediates (**3-6**) has been performed which exhibited
309 some interesting NMR spectral characteristics which have not been reported to date, namely the
310 doubling up of proton and carbon resonances. Our experiments indicate that these effects are due to
311 intermolecular interactions such as dimer formation in combination with hindered rotation. The first
312 single molecule x-ray structure presented in this paper confirmed the synthesis of ZM 241385 (**9**)
313 and provided the basis for the structural comparison with the published protein bound x-ray
314 structure. The overlay of the ZM 241385 (**9**) coordinates revealed that the tyramine portion of the
315 molecule can easily adopt different conformations due to its inherent flexibility. Conformational
316 analyses in vacuum and in explicit aqueous solution allowed an insight into the effect of
317 environment on the conformation.

318

319

320 **Experimental**

321 General Information

322 All reactions were stirred magnetically in oven-dried glassware. Anhydrous solvents were
323 transferred via oven-dried syringe or cannula. Technical grade solvents used for extraction and
324 column chromatography were distilled prior to use. Absolute solvents were used without further
325 purification. Starting materials and reagents **1, 2, 5, 8** and *m*-CPBA were purchased from Aldrich or
326 AK Scientific in the highest available grade and used without further purification. Compound **10**
327 was purchased from Chembridge Support. Compounds **3, 4, 6, 7, 9** and **11** were synthesized in our
328 laboratories. Analytical thin layer chromatography (TLC) plates from Merck were used for reaction
329 control (silica gel 60 on aluminium sheets). Silica gel 60 (Fluka) was used for silica gel flash
330 chromatography. Microwave reactions were performed using a Biotage Initiator 2.0. Proton nuclear
331 magnetic resonance (¹H NMR) spectra and carbon-13 nuclear magnetic resonance (¹³C NMR)
332 spectra were recorded on Bruker spectrometers Advance 400 (400 MHz for ¹H and 101 MHz for
333 ¹³C) at ambient temperature if not stated differently in the solvents indicated and referenced to
334 tetramethylsilane (TMS). Spectra measured at 353 K were referenced to *d*₆-dimethyl sulfoxide
335 (DMSO). Chemical shifts (δ) are reported in parts per million (ppm). Coupling constants (*J*) are
336 reported in Hertz (Hz). The following abbreviations are used: s (singlet), br s (broad singlet), d,
337 (doublet), t (triplet), q (quartet) and m (multiplet). ¹³C NMR spectra were routinely run with
338 broadband decoupling. Low resolution electrospray mass spectra (LRMS) using electrospray
339 ionisation (ESI) were obtained on a Micromass Platform II spectrometer. Unless otherwise stated,
340 cone voltage was 20 eV. High resolution mass spectra (HRMS) were obtained on a Waters LCT
341 Premier XE (TOF) spectrometer fitted with an electrospray ion source. Mass signals are given in
342 mass units per charge (*m/z*). The fragments and intensities are written in brackets. Liquid
343 Chromatography Mass spectra (LCMS) were measured on an Agilent 6100 Series Single Quad
344 LC/MS, Agilent 1200 Series HPLC. (Pump: 1200 Series G1311A Quaternary pump, Autosampler:
345 1200 Series G1329A Thermostatted Autosampler, Detector: 1200 Series G1314B Variable
346 Wavelength Detector). Gradient takes 4 minutes to get to 100% ACN; maintain for 3 minutes and a
347 further 3 minutes to get back to the original 5% ACN. Melting Points were measured with a MP50
348 Melting Point System from Mettler Toledo.

349

350

351 X-ray structure

352 Intensity data for compound **9** was collected on an Oxford Diffraction SuperNova CCD
353 diffractometer using Cu-K radiation, the temperature during data collection was maintained at
354 130.0(1) using an Oxford Cryostream cooling device. The structure was solved by direct methods
355 and difference Fourier synthesis [17]. Thermal ellipsoid plot was generated using the program
356 ORTEP-3 [18] integrated within the WINGX [19] suite of programs.

357

358 Crystal data for Compound **9**. (C₁₆H₁₅N₇O₂)₃(H₂O), *M* = 391.40, *T* = 130.0 K, *d* = 1.54180,
359 Triclinic, space group P-1, *a* = 10.851(2), *b* = 13.349(3), *c* = 15.215(3) Å, *β* = 107.694(19)° =
360 101.122(15)° = 108.736(18)°. *V* 1882.4(6) Å³, *Z* = 4, *D*_c = 1.381 Mg M⁻³, (Cu-K) 0.889 mm⁻¹,
361 *F*(000) = 824 crystal size 0.36 x 0.32 x 0.04 mm³, 12553 reflections measured, 6770 independent
362 reflections [*R*(int) = 0.0353], the final *R* was 0.0539 [*I* > 2 (*I*)] and *wR*(*F*²) was 0.1594 (all data).

363

364 Overlay of X-rays structures

365 The four x-ray structures were overlaid in Maestro 9.2, using only the heterocyclic portion for the
366 superposition. Torsion angles were measured using Maestro 9.2.

367

368 Conformational search of ZM 241385 in vacuo

369 Conformational search was carried out using Macromodel 9.9 in vacuo. The OPLS_2005 force field
370 was used to parameterize the structure. The Polak-Ribiere conjugate gradient method was used to
371 minimize prospective structures. A maximum of 1000 iterations with a convergence threshold of
372 0.1 kcal/mol Å was used for each minimization. The Torsional Sampling method was used to
373 perform the conformational search. Automatic Setup was initially used to identify the search
374 variables, which were subsequently edited. Specifically, torsions within the heterocyclic and furan
375 rings which were automatically selected by Automatic Setup were removed from the search, and all
376 defined ring closures and torsion check parameters were removed. Extended torsion sampling was
377 used, and mirror image conformations were not retained. A maximum of 14000 conformational
378 search steps were set, corresponding to 2000 steps per rotatable bond. No limit was specified on the
379 number of structures saved by the search. An energy window of 6 kcal/mol (25.1 kJ/mol) was
380 specified for saving structures.

381

382 Explicit solvent conformational search of ZM 241385

383 An explicit solvent conformational search of ZM 241385 was performed using HyperChem 7.52,
384 following a previously established procedure [20].

385

386 Synthesis

387 *N''-(Furan-2-ylcarbonyl)carbonohydrazonic diamide (3)*

388 Furoic acid hydrazide (**1**) (6.00 g, 47.5 mmol) and *S*-methylisothiosulfate hemisulfate (**2**) (33.1 g,
389 238 mmol) were added to a solution of sodium hydroxide (3.04 g, 76.1 mmol) in water (150 mL).
390 The clear solution was stirred at room temperature for 24 h and the resultant precipitate was filtered
391 and washed with water and diethyl ether and afterwards dried under vacuum. Product **3** (4.60 g,
392 58%) was obtained as a white solid, mp: 181-184 °C (lit. [9] 213 °C). ¹H NMR (400 MHz, D₂O) δ
393 7.50 (m, 1H, CH-O), 6.87 (m, 1H, CH=C), 6.48 (m, 1H, CH=CH-CH). ¹³C NMR (101 MHz, D₂O)
394 δ 158.5 (C), 155.8 (C), 148.4 (C), 144.4 (CH), 112.4 (CH), 111.5 (CH). LRMS: *m/z* (ESI 20 V)
395 169.2 (MH⁺, 100).

396

397 *5-(Furan-2-yl)-1H-1,2,4-triazol-3-amine (4)*

398 Method A) *N''-(Furan-2-ylcarbonyl)carbonohydrazonic diamide (3)* (1.00 g, 5.95 mmol) was
399 suspended in water (20 mL). The reaction mixture was stirred in the microwave at 140 °C for 1 h
400 (pressure 6 bar) then cooled to room temperature and the solvent was removed under vacuum. The
401 product **4** was obtained as a beige solid (880 mg, 99%). ¹H NMR (400 MHz, *d*₆-DMSO) δ 12.02 (s,
402 br, 1H, NH), 7.69 (dd, *J* = 1.7, 0.7 Hz, 1H, CH-O), 6.69 (d, *J* = 3.2 Hz, 1H, CH=C), 6.54 (dd, *J* =
403 3.3, 1.8 Hz, 1H, CH=CH-CH), 6.01 (br s, 2H, NH₂). ¹³C NMR (101 MHz, *d*₆-DMSO) δ 157.6 (C),
404 151.7 (C), 147.3 (C), 142.7 (CH), 111.3 (CH), 107.7 (CH). LRMS: *m/z* (ESI 20 V) 151.2 (MH⁺,
405 100).

406 Method B) *N''-(Furan-2-ylcarbonyl)carbonohydrazonic diamide (3)* (4.16 g, 24.7 mmol) was
407 suspended in water (85 mL). The reaction mixture was stirred under conventional heating at reflux
408 for 29 h then cooled to room temperature and the solvent was removed under vacuum. The residue
409 was suspended in water (20 mL) and filtered. The filter cake was washed with water and dried
410 under high vacuum. The product **4** (2.96 g, 80%) was obtained as a pinkish white solid, mp: 198-
411 204 °C (lit. [9] 230 °C). ¹H and ¹³C NMR and mass spectral data are in accordance with above
412 characterization.

413

414 *2-(Furan-2-yl)-5-(methylthio)-[1,2,4]triazolo[1,5-a][1,3,5]triazin-7-amine (6)*

415 5-(Furan-2-yl)-1H-1,2,4-triazol-3-amine (**4**) (50.0 mg, 333 μmol) and *N*-
416 cyanodithioiminocarbonate (**5**) (48.7 mg, 333 μmol) were mixed and heated at 170 °C for 1 h
417 under a nitrogen atmosphere. The reaction mixture was cooled to room temperature and absorbed
418 on Celite and purified by column chromatography (dichloromethane: ethyl acetate 95:5 → 85:15).
419 The product **6** (27.0 mg, 32%) was obtained as a white solid, mp: 237-240 °C (lit. [4,11] 238-

420 240 °C). ¹H NMR (400 MHz, *d*₆-DMSO) δ 8.97 (br s, 1H, *NH*), 8.78 (br s, 1H, *NH*), 7.94 (dd, *J* =
421 1.8, 0.8 Hz, 1H, O-*CH*), 7.17 (dd, *J* = 3.4, 0.8 Hz, 1H, C-*CH*), 6.72 (dd, *J* = 3.4, 1.8 Hz, 1H,
422 CH=CH-CH), 2.52 (s, 3H, S-*CH*₃). ¹³C NMR (101 MHz, *d*₆-DMSO) 173.3 (C), 157.2 (C), 156.2
423 (C), 149.6 (C), 145.5 (C), 145.2 (CH), 112.5 (CH), 112.1 (CH), 13.6 (CH₃). LCMS: *m/z* (ESI 20 V)
424 249.1 (MH⁺, 100).

425

426 2-(*Furan-2-yl*)-5-(*methylsulfonyl*)-[1,2,4]triazolo[1,5-*a*][1,3,5]triazin-7-amine (**7**) [4]

427 A solution of *meta*-chloroperoxybenzoic acid (1.06 g, 4.48 mmol) in dichloromethane (10 mL) was
428 added dropwise at -5 °C to a suspension of 2-(*furan-2-yl*)-5-(*methylthio*)-[1,2,4]triazolo[1,5-*a*]
429 [1,3,5]triazin-7-amine (**6**) (278 mg, 1.12 mmol) in dichloromethane (17 mL). The reaction was
430 stirred at room temperature for 22 h before the solvent was removed under vacuum. The crude
431 material was suspended in ethanol (5 mL) and stirred at room temperature for 30 min. The solid was
432 collected by filtration, washed with ethanol and dried to give the title compound **7** (230 mg, 82%)
433 as a white-yellowish solid, mp: 168 °C (dec). ¹H NMR (400 MHz, *d*₆-DMSO) δ 9.81 (s, 1H, *NH*),
434 9.48 (s, 1H, *NH*), 7.99 (dd, *J* = 1.7, 0.8 Hz, 1H, O-*CH*), 7.27 (dd, *J* = 3.4, 0.7 Hz, 1H, C-*CH*), 6.76
435 (dd, *J* = 3.4, 1.8 Hz, 1H, CH=CH-CH), 3.37 (s, 3H, S-*CH*₃); ¹³C NMR (101 MHz, *d*₆-DMSO) 165.3
436 (C), 157.3 (C), 156.8 (C), 152.2 (C), 145.8 (CH), 145.0 (C), 113.4 (CH), 112.3 (CH), 38.9 (CH₃);
437 LCMS: *m/z* (ESI 20 V) 281.0 (MH⁺, 100).

438

439 4-(2-((7-Amino-2-(*furan-2-yl*)-[1,2,4]triazolo[1,5-*a*][1,3,5]triazin-5-yl)amino)ethyl)phenol (**9**)
440 (ZM 241385)

441 Tyramine (**8**) (490 mg, 3.75 mmol) was added to a suspension of 2-(*furan-2-yl*)-5-(*methylsulfonyl*)-
442 [1,2,4]triazolo[1,5-*a*][1,3,5]triazin-7-amine (**7**) (250 mg, 892 μmol) in acetonitrile (25 mL). The
443 reaction mixture was stirred overnight at room temperature. After 22 h the solvent was evaporated,
444 the residue was adsorbed on Celite and purified by column chromatography (dichloromethane:
445 methanol 25:75). The collected fractions with product were evaporated to dryness and recrystallised
446 from ethyl acetate. The title compound **9** (100 mg, 33%) was obtained as a white solid, mp: 229-
447 231 °C (lit. [4] 225-227 °C). ¹H NMR (400 MHz, *d*₆-DMSO, 353 K) δ 8.91 (s, 1H, *OH*), 7.92 (br s,
448 2H, *NH*₂), 7.79 (m, 1H, *H*_{Furan}), 7.14 (br t, 1H, *NH*), 7.04 (m, 3H, 2 *H*_{Ar}, *H*_{Furan}), 6.71 (m, 2H, 2
449 *H*_{Ar}), 6.64 (dd, *J* = 3.3, 1.8 Hz, 1H, *H*_{Furan}), 3.49 (m, 2H, CH₂-CH₂-NH), 2.78 (m, 2H, CH₂-CH₂-
450 NH). ¹³C NMR (101 MHz, *d*₆-DMSO) δ 161.1 (C), 159.0 (C), 155.9 (C), 155.4 (C), 150.1 (C),
451 146.1 (C), 144.1 (CH), 129.1 (CH), 115.0 (CH), 111.4 (CH), 111.2 (CH), 42.4 (CH₂), 33.9 (CH₂).
452 HRMS (C₁₆H₁₅N₇O₂): Calc'd. 338.1360 [M+H]⁺, Found 338.1353. HPLC: *t*_R 7.34 min, 98%
453 (214 nm), 97% (254 nm).

454

455 *[1,2,4]Triazolo[1,5-a][1,3,5]triazin-7-amine (10)*
456 ¹H NMR (400 MHz, *d*₆-DMSO) δ 8.95 (br s, 2H, NH₂), 8.53 (s, 1H, CH-N-C-NH₂), 8.35 (s, 1H,
457 CH); ¹³C NMR (101 MHz, *d*₆-DMSO) δ 159.0 (CH), 156.8 (C), 154.7 (CH), 151.8 (C); LCMS: *m/z*
458 (ESI 20 V) 137.2 (MH⁺, 100).

459

460 *2-(Furan-2-yl)-5-phenethoxy-[1,2,4]triazolo[1,5-a][1,3,5]triazin-7-amine (11)* [4]
461 ¹H NMR (400 MHz, *d*₆-DMSO) δ 8.95-8.60 (2 br s, ratio 1:1, 2H, NH₂), 7.91 (m, 1H, H_{Furan}), 7.32
462 (m, 4H, H_{Ar}), 7.24 (m, 1H, H_{Ar}), 7.14 (dd, *J* = 3.4, 0.5 Hz, 1H, H_{Furan}), 6.71 (dd, *J* = 3.4, 1.8 Hz, 1H,
463 H_{Furan}), 4.52 (t, *J* = 6.8 Hz, 2H, CH₂-O), 3.05 (t, *J* = 6.8 Hz, 2H, CH₂CH₂-O); ¹³C NMR (101 MHz,
464 *d*₆-DMSO) δ 164.9 (C), 158.9 (C), 156.6 (C), 151.6 (C), 145.6 (C), 145.1 (CH), 138.1 (C), 128.9
465 (CH), 128.3 (CH), 126.3 (CH), 112.3 (CH), 112.0 (CH), 67.9 (CH₂), 34.4 (CH₂); HRMS
466 (C₁₆H₁₄N₆O₂): Calc'd. 323.1251 [M+H]⁺, Found 323.1521; mp: 201-204 °C; HPLC: *t*_R 9.14 min,
467 >99.5% (214 nm), >99.5% (254 nm).

468

469 **Accessory Publication**

470 Crystallographic data (excluding structure factors) for the structure reported in this paper has been
471 deposited with the Cambridge Crystallographic Data Centre CCDC 901689. Copies of the data can
472 be obtained free of charge on application to the CCDC, 12 Union Road, Cambridge CB2 1EZ, UK
473 (Fax: +44 1223/336033; deposit@ccdc.cam.ac.uk).

474 ¹H and ¹³C NMR spectra for all synthesized compounds, including HPLC, HRMS and x-ray
475 structure details of ZM 241385 (**9**) are documented in the supplementary information.

476

477 **Acknowledgements**

478 M.J. is a recipient of the Australian Postgraduate Award Industry (APAI). We thank
479 GlaxoSmithKline, GSK R&D China, Singapore for financial support and Dr Jason Dang (Monash
480 University) for assistance in obtaining NMR and HRMS data.

481

482 **References**

- 483 1. Baraldi PG, Cacciari B, Spalluto G, Borioni A, Viziano M, Dioniotti S, Ongini E (1995). *Curr*
484 *Med Chem* 2:707.
- 485 2. Müller CE (2000). *Drug Future* 25:1043.
- 486 3. Richardson PJ, Kase H, Jenner PG (1997). *Trends Pharmacol Sci* 18 (9):338.
- 487 4. Caulkett PWR, Jones G, Collis MG, Poucher SM (1991). *European Patent EP 459702*.
- 488 5. Jaakola V-P, Griffith MT, Hanson MA, Cherezov V, Chien EYT, Lane JR, IJzerman AP, Stevens
489 RC (2008). *Science* 322 (5905):1211.
- 490 6. Doré AS, Robertson N, Errey JC, Ng I, Hollenstein K, Tehan B, Hurrell E, Bennett K, Congreve
491 M, Magnani F, Tate CG, Weir M, Marshall FH (2011). *Structure* 19 (9):1283.
- 492 7. Minetti P, Tinti MO, Carminati P, Castorina M, Di Cesare MA, Di Serio S, Gallo G, Ghirardi O,
493 Giorgi F, Giorgi L, Piersanti G, Bartoccini F, Tarzia G (2005). *J Med Chem* 48 (22):6887.
- 494 8. Federico S, Paoletta S, Cheong SL, Pastorin G, Cacciari B, Stragliotto S, Klotz KN, Siegel J, Gao
495 Z-G, Jacobson KA, Moro S, Spalluto G (2011). *J Med Chem* 54 (3):877.
- 496 9. Srivastava RP, Kumar VV, Bhatia S, Sharma S (1995). *Indian J Chem* 34B:209.
- 497 10. Dolzhenko AV, Pastorin G, Dolzhenko AV, Chui WK (2009). *Tetrahedron* 50:2124.
- 498 11. Caulkett PWR, Jones G, McPartlin M, Renshaw ND, Stewart SK, Wright B (1995). *J Chem Soc*
499 *Perkin Trans* 1:801.
- 500 12. Kessler H (1970). *Angew Chem Int Ed* 9:219.
- 501 13. Lunazzi L, Macciantelli D, Grossi L (1983). *Tetrahedron* 39 (2):305.
- 502 14. Anderson JE, Grimth DL, Roberts JD (1969). *J Am Chem Soc* 91:6371.
- 503 15. Zhukov A, Andrews SP, Errey JC, Robertson N, Tehan B, Mason JS, Marshall FH, Weir M,
504 Congreve M (2011). *J Med Chem* 54 (13):4312.
- 505 16. Jaakola V-P, Griffith MT, Hanson MA, Cherezov V, Chien EYT, Lane JR, IJzerman AP,
506 Stevens RC (2008). *Science* 322:1211.
- 507 17. Sheldrick G (2008). *Acta Crystallogr A* 64 (1):112.
- 508 18. Farrugia LJ (1997). *J Appl Crystallogr* 30 (5-1):565.
- 509 19. Farrugia LJ (1999). *J Appl Crystallogr* 32 (4):837.
- 510 20. Yuriev E, Kong DCM, Iskander MN (2004). *Eur J Med Chem* 39 (10):835.
- 511 21. Capuano B, Crosby IT, Forsyth CM, McRobb FM, Moudretski VV, Taylor DA, Vom A, Yuriev
512 E (2010) *Struct Chem* 21 (3):613.
- 513 22. Golzarroshan B, Siddegowda MS, Li HQ, Yathirajan HS, Narayana B, Rathore R.S (2012) *J*
514 *Mol Struct* 1018:107.

515